Hole subband structure in a semiconductor quantum well revisited

L. Diago-Cisneros
Departamento de Física Aplicada, Facultad de Física, Universidad de La Habana
Vedado 10400, Ciudad de La Habana, Cuba

H. Rodríguez-Coppola and R. Pérez-Alvarez
Departamento de Física Teórica, Facultad de Física, Universidad de La Habana
Vedado 10400, Ciudad de La Habana, Cuba

Recibido el 16 de julio de 1999; aceptado el 6 de marzo de 2000

The hole subband structure, the band mixing effects and the symmetry properties of the states in a [100] GaAs quantum well are given for the case of infinite potential barriers, in the framework of the Kohn-Lüttinger model using the Full Transfer Matrix technique. The calculations demand not too much computational effort and are in good agreement with experimental results. Our labelling of the states, performed according to the dominant contribution at $k_T = 0$, where the states are pure light and heavy hole states, agrees with that presented by Chang and Schulman at variance with that of other authors. The band mixing away from the Brillouin Zone center leads to changes in the contributions of the light and heavy hole components to each state.

Keywords: Hole states; band mixing; discrete symmetries

Para el caso de un pozo cuántico infinito [100] de GaAs, se presentan la estructura de subbandas y los efectos de la mezcla de las bandas en las propiedades de simetría de los estados, en el marco del modelo Kohn-Lüttinger usando la técnica de la Matriz de Transferencia Completa. Los cálculos no exigen mucho esfuerzo de cómputo y están en buena concordancia con resultados experimentales. Nuestro etiquetado de los estados, realizado de acuerdo con la contribución dominante en $k_T = 0$, donde los estados de huecos pesados y ligeros son puros, coincide con el propuesto por Chang y Schulman pero difiere del de otros autores. La mezcla de los estados lejos del centro de la zona de Brillouin conduce a cambios en las contribuciones de las componentes de huecos pesados y ligeros a cada estado.

Descriptores: Estados de huecos; mezcla de las bandas; simetrías discretas

PACS: 73.20.Dx; 71.55.Eq

1. Introduction

The dispersion relation of the hole subbands in quasi-two dimensional (Q2D) heterostructures made of III-V and II-VI materials has received substantial attention in the last ten years. Theoretical calculations show the highest hole band to have a low effective mass in both strained and unstrained systems [1] and, in addition, show a highly nonparabolic subband dispersion near the Valence band maximum [1, 2]. These effects have potential significant practical interest in new devices. In recent years several theoretical calculations were made in Q2D systems analyzing the hole subbands because the band mixing between heavy and light hole bands in GaAs-AlGaAs systems. Most of them use $\kappa \cdot \mathbf{p}$ Hamiltonians in different schemes [1–12].

The Kohn-Lüttinger (KL) model Hamiltonian is a practical one to study the hole subbands in these materials and it is flexible in including external perturbations such as external fields [7, 12] and strain [1]. The main effect of this model Hamiltonian for those materials is the mixing of light and heavy hole bands away from the Γ point which substantially affects the optical properties [5] of systems made of such materials.

The hole subband structure in quantum wells (QW) has been previously studied with a Kohn-Lüttinger Hamiltonian [4, 7, 9, 10, 12]. While these studies have added substantial contributions to the elucidation of this problem, there remain some aspects which do not appear to have received sufficient attention and/or which because of their interest deserve further clarification. These are essentially of three types, namely: (1) The effect of the discrete symmetries when the initially 4×4 Hamiltonian is block-diagonalized by appropriate transformations and the consequences of this on the wavefunctions of the states of the subspaces of solutions thus obtained. (2) The labelling of the hole states of the QW. This would seem to require an explanation—not always clarified—of the criteria on which the labelling is based for different values of the 2D in-plane wavevector and, in any case, it should be consistent with the conclusions of the calculations based on tight-binding schemes [5], which is not always the case. (3) Various techniques have been employed for the numerical calculations [4, 7, 9, 10, 12] which appear to be useful and efficient but their practical usefulness for other potential users would improve if some technical details of instrumental significance for their implementation were explained. The aim of this paper is to address such questions.

For all these issues it suffices to study the case of a quantum well with infinite barriers (iQW). We shall study a GaAs well grown in the [100] direction, start from a

4×4 Hamiltonian and employ a Full Transfer Matrix (FTM) technique [13–15], different from the usual Transfer Matrix method which involves only amplitudes [16].

The remaining parts of this paper are organized as follows: Sect. 2 presents the FTM in the case of a KL model Hamiltonian for flat band potential, in Sect. 3 a description of the main discrete symmetries of the KL Hamiltonian is given together with their consequences for the states. Section 4 gives the dispersion relation and the squared wavefunction of the iQW in the axial approximation and Sect. 5 gives the numerical results together with its analysis. Finally some conclusions are presented in sect. 6.

2. TM for flat band KL model

The infinite-potential barrier case of a GaAs QW, grown in the [100]-direction, considered as the z axis is analyzed. A detailed analysis of the form of the KL Hamiltonian for different directions in the structure is given in [10]. In this paper the assumptions, conventions and notation used by Broido and Sham [4] were used, particularly the order in the basis functions for the $\kappa \cdot \mathbf{p}$ Hamiltonian. Then taking into account symmetry considerations [17], the KL Hamiltonian to deal with is

$$\hat{\mathbf{H}}_o = \begin{vmatrix} P+Q & R-T' & -S+\frac{1}{\sqrt{3}}T^* & T \\ R^*-T'^* & P-Q & -T & S+\frac{1}{\sqrt{3}}T^* \\ -S^*+\frac{1}{\sqrt{3}}T & -T^* & P-Q & R+T' \\ T^* & S^*+\frac{1}{\sqrt{3}}T & R^*+T'^* & P+Q \end{vmatrix}. \quad (1)$$

Here and throughout the paper k_x, k_y, k_z denote Bloch wavevector components and γ_1, γ_2, γ_3 the Lüttinger parameters. The variables P, Q, R, T, T' and S are given in Appendix A.

The usual case $\beta = 0$, whose validity was amply discussed in Ref. 4, is considered. A unitary transformation [4] rearranges the order of the states and separates them in two blocks according to their Kramer degeneracy, so the Hamiltonian (1) is block-diagonalized into two 2×2 blocks, which are labeled "up" (U) and "low" (L) in analogy with electron spin.

$$\hat{\mathbf{H}}'_o = \begin{vmatrix} \hat{\mathbf{H}}^{\mathrm{U}} & 0 \\ 0 & \hat{\mathbf{H}}^{L} \end{vmatrix}, \quad (2)$$

where the blocks are given by

$$\hat{\mathbf{H}}^{U} = \begin{vmatrix} A_1\kappa_T^2 + B_2\hat{k}_z^2 + V(z) - E & C_{xy} - iD_{xy}\hat{k}_z \\ C_{xy} + iD_{xy}\hat{k}_z & A_2\kappa_T^2 + B_1\hat{k}_z^2 + V(z) - E \end{vmatrix}, \quad (3)$$

$$\hat{\mathbf{H}}^{L} = \begin{vmatrix} A_2\kappa_T^2 + B_1\hat{k}_z^2 + V(z) - E & C_{xy} - iD_{xy}\hat{k}_z \\ C_{xy} + iD_{xy}\hat{k}_z & A_1\kappa_T^2 + B_2\hat{k}_z^2 + V(z) - E \end{vmatrix}, \quad (4)$$

and $\hat{k}_z = -i\,(d/dz)$. Expressions for A_1, A_2, B_1, B_2, C_{xy}, D_{xy} and k^2 are given in Appendix A. Here and henceforth, hole energy is counted as positive. For the eigenvalue problem

$$\left\{\hat{\mathbf{H}}^{U,L}(\kappa, E)\right\} \varphi_{u,l}(\mathbf{r}) = 0. \quad (5)$$

Due to translational symmetry in the (x, y) plane of the system, the solutions of (3) and (4) are written in the usual form

$$\varphi_{u,l}(\mathbf{r}) = e^{i(k_x x + k_y y)}\varphi_{u,l}(z) = e^{i(k_x x + k_y y)} \begin{vmatrix} g_{1,3}(z) \\ g_{2,4}(z) \end{vmatrix}. \quad (6)$$

Since the secular determinant of (5) is the same for both U and L Hamiltonians, the eigenvalues are equal so, for the sake of illustration, hereafter the U case will be considered. In the flat band case the solution (6) can be written as:

$$\begin{vmatrix} g_1(z) \\ g_2(z) \end{vmatrix} = e^{i\lambda z} \begin{vmatrix} h_1 \\ h_2 \end{vmatrix}. \quad (7)$$

From (3) and (5)–(7), the algebraic system of equations for the flat band potential is:

$$\begin{vmatrix} A_1\kappa^2 + B_2\lambda^2 + \mathcal{E} & C_{xy} - iD_{xy}\lambda \\ C_{xy} + iD_{xy}\lambda & A_2\kappa^2 + B_1\lambda^2 + \mathcal{E} \end{vmatrix} \begin{vmatrix} h_1 \\ h_2 \end{vmatrix} = 0, \quad (8)$$

where $\mathcal{E} = V_0 - E$; V_0 is a constant.

From the zeros of the secular determinant of (8), one can obtain non trivial solutions. The fundamental magnitudes to use are taken in atomic units with a_0 taken as the Bohr's radius and Ry as the Rydberg constant.

Now the determinant of (8) reads (in atomic units)

$$\begin{vmatrix} a_1 q_T^2 + b_2 q^2 + \tilde{\mathcal{E}} & t_{xy} - iS_{xy}q \\ t_{xy} + iS_{xy}q & a_2 q_T^2 + b_1 q^2 + \tilde{\mathcal{E}} \end{vmatrix} = 0, \quad (9)$$

which is a fourth-order polynomial equation, whose solutions are

$$\begin{aligned} q_1 &= \sqrt{\frac{1}{\alpha_T}\left(\sqrt{\beta_T^2 - \alpha_T\delta_T} - \beta_T\right)}, \\ q_2 &= -q_1, \\ q_3 &= \sqrt{\frac{1}{\alpha_T}\left(-\sqrt{\beta_T^2 - \alpha_T\delta_T} - \beta_T\right)}, \\ q_4 &= -q_3. \end{aligned} \quad (10)$$

For the definitions of $a_1, a_2, b_1, b_2, q_T, q, \tilde{\mathcal{E}}, S_{xy}, t_{xy}, \alpha_T$ and β_T see Appendix A. With the aforementioned values (10), one can find the solutions as

$$\varphi_{uj}(z) = \Lambda_{uj} e^{iq_j z} \begin{vmatrix} a_2 q_T^2 + b_1 q_j^2 + \tilde{\mathcal{E}} \\ -(t_{xy} + iS_{xy}q_j) \end{vmatrix}; \quad j = 1, 2, 3, 4, \quad (11)$$

as the linearly independent solutions for the flat band case, where Λ_{uj} is the normalization constant, which can be written as

$$|\Lambda_{uj}|^2 = \frac{1}{2\pi} \frac{1}{\left[a_2 q_T^2 + b_1\left(q_{Rj}^2 - q_{Ij}^2\right) + \tilde{\mathcal{E}}\right]^2 + 4b_1 q_{Rj}^2 q_{Ij}^2 + (t_{xy} - iS_{xy}q_j)(t_x + iS_{xy}q_j)}.$$

To introduce the FTM one defines the two-component supervector [13]

$$\Phi_u(z) = \begin{vmatrix} \varphi_u(z) \\ \varphi'_u(z) \end{vmatrix}. \tag{12}$$

The FTM $\mathbf{M}^U(z_1, z_o)$ can be defined as the 2×2 supermatrix, which transfers any solution $\Phi_u(z)$ from z_o to z_1 [14], *i.e.*,

$$\Phi_u(z_1) = \mathbf{M}^U(z_1, z_o) \cdot \Phi_u(z_o). \tag{13}$$

To obtain $\mathbf{M}^U(\xi_1, \xi_o)$, where $\xi_1 = z_1/a_o$ and $\xi_o = z_o/a_o$ the following expression can be applied [13]:

$$\mathbf{M}^U(\xi_1, \xi_o) = \mathbf{N}(\xi_1) \cdot \mathbf{N}(\xi_o)^{-1}, \tag{14}$$

Where $\mathbf{N}(\xi)$ is a matrix of the linearly independent solutions of the system of equations. It can be cast as

$$\mathbf{N}(\xi) = \begin{vmatrix} h_{11}e^{iq_1\xi} & h_{12}e^{iq_2\xi} & h_{13}e^{iq_3\xi} & h_{14}e^{iq_4\xi} \\ h_{21}e^{iq_1\xi} & h_{22}e^{iq_2\xi} & h_{23}e^{iq_3\xi} & h_{24}e^{iq_4\xi} \\ iq_1h_{11}e^{iq_1\xi} & iq_2h_{12}e^{iq_2\xi} & iq_3h_{13}e^{iq_3\xi} & iq_4h_{14}e^{iq_4\xi} \\ iq_1h_{21}e^{iq_1\xi} & iq_2h_{22}e^{iq_2\xi} & iq_3h_{23}e^{iq_3\xi} & iq_4h_{24}e^{iq_4\xi} \end{vmatrix}. \tag{15}$$

By substitution of (15) in (14) and performing the corresponding matrix operations, the following structure for the FTM elements can be obtained

$$M_{ij}^U(\xi_1, \xi_o) = \frac{1}{\Delta_T}\left[\ell_{ij}^{(1)}\cos(\tilde{q}_1) + \ell_{ij}^{(2)}\cos(\tilde{q}_3) + \ell_{ij}^{(3)}\sin(\tilde{q}_1) + \ell_{ij}^{(4)}\sin(\tilde{q}_3)\right], \tag{16}$$

where we used $\tilde{q}_i = q_i(\xi_1 - \xi_o)$; $i = 1, 3$. The matrix elements coefficients for $M_{ij}^U(\xi_1, \xi_o)$ are given in Appendix B.

3. Discrete symmetry properties of the KL Hamiltonian

When studying the KL Hamiltonian it is useful to take advantage of the discrete symmetries it has. As pointed out in Ref. 7, the two basic discrete symmetry properties are the time reversal invariance (TR) and the inversion of coordinate z (IC) without changing the value of the in-plane wavevector.

The basis set used in Ref. 7 was different from the one used here. The TR operator on the basis of Ref. 7 is given by $\hat{\mathbf{K}}_{\rm APB} = \Sigma_y \hat{K}_o$, where

$$\Sigma_{\rm y} = \begin{vmatrix} \mathbf{0} & \sigma_y \\ \sigma_y & \mathbf{0} \end{vmatrix}.$$

Here the APB subscript corresponds to operators given in the basis of Ref. 7, while the subscript BS will correspond to our basis, which we recall is that of Ref. 4. Here and henceforth σ_x, σ_y and σ_z are the Pauli matrices and $\hat{K}_o \cdot \hat{\mathbf{V}}$ indicates the complex conjugate—not the Hermitian conjugate of any operator $\hat{\mathbf{V}}$.

It is necessary, then, to change the order of the basis function used from APB to BS. The matrix to do this operation is:

$$\mathbf{T} = \begin{vmatrix} -1 & 0 & 0 & 0 \\ 0 & 0 & 1 & 0 \\ 0 & i & 0 & 0 \\ 0 & 0 & 0 & -i \end{vmatrix}, \tag{17}$$

which leads to the following form for the TR operator:

$$\hat{\mathbf{K}}_{\rm BS} = \begin{vmatrix} \mathbf{0} & \sigma_x\hat{K}_o \\ -\sigma_x\hat{K}_o & \mathbf{0} \end{vmatrix}. \tag{18}$$

Using (18) on the KL Hamiltonian we have $\hat{\mathbf{K}}_{\rm BS}\hat{\mathbf{H}}_o\hat{\mathbf{K}}_{\rm BS}^{-1} = \hat{\mathbf{H}}_o\hat{\mathbf{K}}_o$. Here and henceforth $\mathbf{0}$ is the 2×2 null matrix.

Consider now the unitary transformation $\mathbf{U}$ [4] that block-diagonalizes the KL Hamiltonian (1), *i.e.*, which allows to analyze the system of equations as two different but spatially equivalent sub-systems with smaller matrices. The operator $\hat{\mathbf{K}}_{\rm BS}$ conmutes with $\mathbf{U}$ and separates the states "Kramer +" (U Hamiltonian) and "Kramer −" (L Hamiltonian) to time reversal (it is not difficult to show that the transformation $\mathbf{U}$ is related to the TR operation). Then the KL Hamiltonian (1) is invariant under TR and every sub-space of it has a definite value of Kramer degeneracy.

The initially 4×4 KL Hamiltonian is also invariant under IC operation [7], which corresponds to a change of sign of the z coordinate only without changing the value of the in-plane wavevector. This operation corresponds to inverting all coordinates and performing a rotation through π in the (x, y) plane. Performing the operation of changing the $\boldsymbol{\kappa} \cdot \mathbf{p}$ basis to ours, the operator for IC given in Ref. 7, takes the following

expression:

$$\hat{\sigma}_{\rm BS} = \begin{vmatrix} -\mathbf{I}_2 & \mathbf{0} \\ \mathbf{0} & \mathbf{I}_2 \end{vmatrix}, \tag{19}$$

where $\mathbf{I}_2$ is the 2×2 identity matrix. From (19) it can be readily seen that $\hat{\sigma}_{\rm BS}$ is unitary and its application reads: $\hat{\sigma}_{\rm BS}\hat{\mathbf{H}}_o(-z)\hat{\sigma}_{\rm BS} = \hat{\mathbf{H}}_o(z)$. This operation produces in the wavefunction the following result: $\hat{\sigma}_{\rm BS}\Psi(-z) = p\Psi(z)$ with $p = \pm 1$, denoting the parity. It is worth noticing that the parities of the components of the supervector are opposite, *i.e.*,

- For $p = +1$ it is

$$\begin{vmatrix} \Psi_1(z) \\ \Psi_2(z) \end{vmatrix} = \begin{vmatrix} -\Psi_1(-z) \\ \Psi_1(-z) \end{vmatrix}.$$

- For $p = -1$ it is

$$\begin{vmatrix} -\Psi_1(z) \\ -\Psi_2(z) \end{vmatrix} = \begin{vmatrix} -\Psi_1(-z) \\ \Psi_1(-z) \end{vmatrix}.$$

Considering the transformation $\mathbf{U}$ that block-diagonalizes the Hamiltonian, it can be shown that

$$\mathbf{U}\hat{\mathbf{H}}_o(z)\mathbf{U}^{-1} = \mathbf{U}\hat{\sigma}_{\rm BS}\hat{\mathbf{H}}_o(-z)\sigma_{\rm BS}\mathbf{U}^{-1} = \hat{\mathbf{H}}'_o(-z). \tag{20}$$

Due to the fact that the operations $\hat{\sigma}_{\rm BS}$ and $\mathbf{U}$ do not commute, it is not possible to keep the symmetry under IC in the 2×2 sub-spaces U and L away from the Γ point, although the whole 4×4 Hamiltonian keeps always the IC symmetry. Once the block-diagonalization is performed, the operator $\hat{\sigma}_{\rm BS}$ changes to

$$\mathbf{U}\hat{\sigma}_{\rm BS}\mathbf{U}^{-1} = \hat{\Gamma}_{\rm BS} = \begin{vmatrix} \mathbf{0} & -\sigma_x \\ -\sigma_x & \mathbf{0} \end{vmatrix}, \tag{21}$$

where $\hat{\Gamma}_{\rm BS}$ is a unitary operator. Equation (20) can be cast as

$$\hat{\mathbf{H}}'_o(z) = \hat{\Gamma}_{\rm BS}\hat{\mathbf{H}}'_o(-z)\hat{\Gamma}_{\rm BS}, \tag{22}$$

which gives the following relations:

$$\begin{aligned} \hat{\mathbf{H}}^{\rm U}(z) &= \sigma_x\hat{\mathbf{H}}^{\rm L}(-z)\sigma_x, \\ \hat{\mathbf{H}}^{\rm L}(z) &= \sigma_x\hat{\mathbf{H}}^{\rm U}(-z)\sigma_x. \end{aligned} \tag{23}$$

Relations (23) show explicitly that the sub-spaces U and L are not invariant under IC for a non-zero value of κ_T.

At $\kappa_T = 0$, on the other hand, both Hamiltonians U and L are diagonal and thus invariant under the IC operation. The matrix σ_z performs the IC operation and leads to the following symmetry property of the sub-space wavevector $\sigma_z\Psi_{\rm U,L}(-z) = p\Psi_{\rm U,L}(z)$. This shows that the two components of the wave-vector in each sub-space have opposite parities. This analysis supports the results given in Ref. 12 and in this paper, where the square of the wavefunctions depicted in their figures and in ours later, are not symmetric with respect to the well center at any $\kappa_T \neq 0$, but are symmetrical at $\kappa_T = 0$.

Then, for the hole subbands given for one sub-space of the KL Hamiltonian, the Γ point is a particular one where the states decouple in the case of no external field or strain, given independent series of states for heavy and light holes with parity defined. When moving away from the Brillouin zone center, the mixing of the bands leads to a lack of IC symmetry of the states of the components 2×2 sub-spaces, even though the whole 4×4 state remains symmetric.

Relations (23) allow one to find the symmetry transformation of the envelope functions and the TM. It can easily be deduced that the TM fulfils the equality

$$\Sigma_x\mathbf{M}^{\rm U,L}(-z,-z_o)\Sigma_x = \mathbf{M}^{\rm L,U}(z,z_o), \tag{24}$$

where

$$\Sigma_x = \begin{vmatrix} \sigma_x & \mathbf{0} \\ \mathbf{0} & \sigma_x \end{vmatrix}.$$

4. Dispersion relation and local spectral strength for the iQW

Let us now study the states of the iQW with the KL Hamiltonian given for one of the 2×2 subspaces, say U for instance. To obtain the trascendental equation for the dispersion relation of the iQW the following boundary conditions must be satisfied:

$$\Phi_u(0) = \begin{vmatrix} 0 \\ \varphi'_u(0) \end{vmatrix}; \qquad \Phi_u(L_w) = \begin{vmatrix} 0 \\ \varphi'_u(L_w) \end{vmatrix}. \tag{25}$$

Using (25) with TM, the secular determinant for the states can be written as

$$M_{13}(L_w,0)M_{24}(L_w,0) - M_{23}(L_w,0)M_{14}(L_w,0) = 0, \tag{26}$$

which after some algebra can be cast as

$$\sin\tilde{q}_1 \sin\tilde{q}_3 = \frac{2\left[1 - \cos\tilde{q}_1\cos\tilde{q}_3\right]}{\left(\frac{t_{xy}}{S_{xy}}\right)^2\left(\frac{1}{q_1q_3}\right)\left(\sqrt{\frac{\alpha_1}{\alpha_2}} - \sqrt{\frac{\alpha_2}{\alpha_1}}\right) + \left(\frac{\alpha_1q_3}{\alpha_2q_1} + \frac{\alpha_2q_1}{\alpha_1q_3}\right)}. \tag{27}$$

Expressions for α_1 and α_2 are given in Appendix B.

Some algebra shows (27) to be identical to that derived in Ref. 3 for the Γ point.

Turning now to the important case $k_T = 0$, this limit must be taken in (27). To do so, one considers that $\tilde{\mathcal{E}}(q_T, q_z)$ is an even function of q_T and hence the function $\nabla_{q_T}\tilde{\mathcal{E}}(q_T, q_z)$ has

to be odd. Then at $q_T = 0$ we have $\hat{\mathbf{p}}_o = \text{const}$ [18], which leads to

$$\frac{q_1^2}{q_3^2}\left(\frac{\gamma_1 + 2\gamma_2}{\gamma_1 - 2\gamma_2}\right) = \frac{\tilde{\mathcal{E}}_{\text{LH}}}{\tilde{\mathcal{E}}_{\text{HH}}}. \tag{28}$$

Considering a parabolic approximation to the dispersion law for the heavy and light holes bands in this limit, the energy can be cast as

$$\tilde{\mathcal{E}}_{\text{HH}} = (\gamma_1 - 2\gamma_2)\, q_3^2, \tag{29}$$
$$\tilde{\mathcal{E}}_{\text{LH}} = (\gamma_1 + 2\gamma_2)\, q_1^2.$$

From (29) and (28),

$$q_1^2 = q_3^2, \tag{30}$$

at $q_T = 0$.

One has to ensure that (27) is not a trivial identity in this limit. One has

$$\lim_{q_T \to 0}\left(\frac{t_{xy}}{S_{xy}}\right) = 0;$$

$$\lim_{q_T \to 0}\left(\frac{\alpha_1 q_3}{\alpha_2 q_1} + \frac{\alpha_2 q_1}{\alpha_1 q_3}\right) \approx 2,97,$$

which eliminate this possibility.

Also, by using condition (30) and also $\tilde{q} = \pi n$, it is easy to see that

$$\lim_{q_T \to 0}\left(1 - \cos^2 \tilde{q}\right) = 0; \quad \lim_{q_T \to 0}\left(\sin^2 \tilde{q}\right) = 0,$$

which excludes the possibility of turning (30) into a trivial identity.

Using (27) in the resulting expression in this limit we obtain

$$\sin^2 \tilde{q} = 0,$$

which leads to the uncoupled series of levels

$$E_{\text{HH}} = \frac{\hbar^2}{2m_o}(\gamma_1 - 2\gamma_2)\left(\frac{\pi n}{L_w}\right)^2,$$
$$E_{\text{LH}} = \frac{\hbar^2}{2m_o}(\gamma_1 + 2\gamma_2)\left(\frac{\pi n}{L_w}\right)^2, \tag{31}$$

a which unambiguously label the hole subbands as heavy (larger effective mass) and light (smaller mass) at the center of the Brillouin zone.

As in the case of finite barriers the secular equation can be cast in a form similar to (26) (see Ref. 13), the similar individual series for heavy and light hole states can be obtained.

On letting κ_T grow from the initial zero value we identify unambiguously the HH and LH bands. The infinite barrier simplification allow us to follow up this issue analytically but any lowering of the barriers to real life values cannot in practice alter the relative ordering of the energy levels, at least for the lower values of the quantum index n, which are usually the ones that matter for most physical properties.

To study the mixing of holes the square modulus of the wavefunction was evaluated by using the FTM representation of the state. This gives

$$\mathcal{D}^{\text{U}}(\tilde{\mathcal{E}}, q_T, \xi) = \left[\mathbf{M}^{\text{U}}_{\text{AD}}(\xi, \xi_o)\Phi'(\xi_o)\right]^{\dagger} \times \left[\mathbf{M}^{\text{U}}_{\text{AD}}(\xi, \xi_o)\Phi'(\xi_o)\right]. \tag{32}$$

We considered boundary conditions (25) in (32). Then, the mixed terms vanish and an expression with explicit heavy-hole and light-hole contributions is derived:

$$\mathcal{D}^{U} = \mathcal{D}^{\text{U}}_{\text{HH}} + \mathcal{D}^{\text{U}}_{\text{LH}} \tag{33}$$

Also the square modulus of the wavefunction of L states was evaluated. Taking advantage of the symmetries described above, we obtain the relation

$$\mathcal{D}^{L}(\tilde{\mathcal{E}}, q_T, \xi) = \mathcal{D}^{U}(\tilde{\mathcal{E}}, q_T, -\xi). \tag{34}$$

5. Numerical results

To determine the dispersion relation of the hole states in the iQW the Eq. (27) must be numerically evaluated. As usual this is written as

$$Z(q_1, q_3) = \sin \tilde{q}_1 \sin \tilde{q}_3 - f\left(\tilde{q}_1, \tilde{q}_3, q_1, q_3\right), \tag{35}$$

where $f\left(\tilde{q}_1, \tilde{q}_3, q_1, q_3\right)$ is the right-hand side of Eq. (27). Function $Z(q_1, q_3)$ is generally a strong nonlinear, two-dimensional and complex-valued function whose zeros we are looking for.

Methods for root finding are formally divided into zero-searching techniques and minimum-searching techniques. In the first category the most common method is the Newton-Raphson (NR) [23].

Taking into account the complex character of (35) one can separate its real and imaginary parts and explicitly write the corresponding nonlinear system of equations involved. There are no good universal methods for solving systems of two or more nonlinear equations, due to the fact that both $Z_{\Re}$ and $Z_{\Im}$ are two arbitrary unrelated functions. They have zero contour lines that divide the plane (q_1, q_3) into regions. In Fig. 1 a typical situation is sketched.

Although the NR provides a very efficient convergence process provided one has an educated initial guess and well behaved functions in the system of equations, this is not our case because even though the educated initial guess can be obtained from the series (31) for the iQW at the Γ point, the functions of the system (35) are not well behaved. Then the NR badly fails to converge. So, it is necessary to resort to minimum searching techniques. The procedure is to start with the initial guess at $q_T = 0$, mentioned before to define a box in which the zero is located. At a new value of q_T the solution just obtained for the previous one is used as the new guess to find the new box. This procedure is called "follow the box".

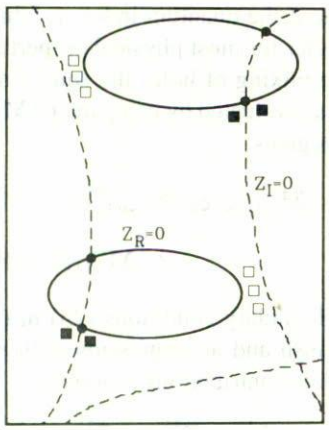

FIGURE 1. Schematic representation of the zero-contour boundaries of functions $Z_{\Re}$ and $Z_{\Im}$. Solid curves refer to $Z_{\Re}(q_1, q_3)$, dashed curves to $Z_{\Im}(q_1, q_3)$, which the real and imaginary parts of function Z given by (27). Each contour line divides (q_1, q_3) plane into positive and negative regions. The desired solutions (global minima) are the intersections of these unrelated zero curves. The circles correspond to global minima, the filled rectangles correspond to local minima and the non-filled ones refer to isolated minima.

There are points of accidental degeneracy in the dispersion relation where the assignation becomes ambiguous. To overcome this difficulty a change in the procedure must be effected. Instead of the procedure "follow the box", a mapping of all extrema of the system of equations must be used [19]. These extrema include maxima, global minima, local and isolated minima (See Fig. 1 for every kind of extrema). To determine the accuracy of the determination of such extrema the function Z_{MOD} is evaluated [23], which is the modulus of function (35).

The desired solutions are the global minima, because the local and isolated minima are the wing bands [20] which are a consequence of the incomplete basis representing the $\kappa \cdot \mathbf{p}$ functions used.

For actual solutions the accuracy obtained, determined by the value of Z_{MOD} was within 10^{-14}–10^{-16} and for isolated minima it was within 10^{-4}–10^{-6}. This difference allows one to properly determine the actual solutions.

For the determination of the dispersion relation the zero of energy was taken at the top of the bulk valence band of GaAs and the values for the Lüttinger parameters were taken from [4]. In the computation there were several points for which the accuracy achieved for actual solutions decreases with respect to the interval mentioned above for determined ranges of values of q_T, although higher than the accuracy for local and isolated minima. This is presumably due to a stronger interaction between light and heavy hole bands in this range.

As will be seen in all dispersion figures, our dispersion curves are always higher in energy than those obtained for the fQW of the same width, as expected, but the same overall look is always obtained. The figures show several standard features such as nonparabolicity, the anisotropy in the in-plane dispersion and the saddle point behavior of subbands HH2 and HH3 at Γ point [2, 3].

In some numerical studies of essentially the same system as studied here [7, 9, 12], a different ordering of the states appears to be obtained, with HH2 and LH1 interchanged with respect to the present results. We note, however, that the labelling proposed for the different states is in these cases assigned without any explanatory criterion to the numerical results obtained in the calculation, while in the tight binding calculation of [1, 6] the LH or HH assignments are explained and interpreted—albeit in a different scheme from ours—and the ordering thus obtained is identical to that of the results obtained here.

Another general result can be seen from our figures. For all well widths the bands of states LH1 and HH3 appear to cross each other. This "crossing" is obtained by analyzing the full extrema picture and this result, although expressed in Ref. 6 explicitly, is not reflected in the curves of their Fig. 1, in which they obtained an anticrossing point. Our calculation, based on the study of the square modulus of the wavefunction allow us to determine whether a crossing or anticrossing occurs. On general grounds it can be stated that the point must be of anticrossing since for the point group of the KL Hamiltonian (D_{4h}), at $q_T = 0$ corresponds the group C_{2V}, whose double group has only the irreducible representation L_5 which have states of the same symmetry, so they must anticross.

Noticing that for the iQW of 120 Å in the range $0 < \kappa_T < 0,0178$ Å^{-1} the function $Z(q_1, q_3)$ is strictly real, the NR technique can be used in this range. This validates the strategy "follow the box" used because a complete agreement was achieved by both techniques for that case.

In Figs. 4–6 the components of the square modulus of the wavefunction of different states are depicted for both the U and L subspaces. They show the IC symmetry of the states whether corresponding to the Γ point (Fig. 4) and the absence of it at any other point (Figs. 5 and 6), and also the complementary shifting for states of the U and L states.

In Fig. 2a the first four hole subbands for a GaAs iQW of 50 Å are presented along the $\langle 10 \rangle$ in-plane direction. Our labelling derived unambiguously from series (31) is coincident with that proposed in [1, 6] and differs from that reported by others authors in [7, 9, 12] who interchange the labels of the states HH2 and LH1. Subbands LH1 and HH3 "anti-cross" each other at the point $\kappa_T = 0,055841$ Å^{-1}. It also depicts the hole valence band structure reported in [12] for a fQW case and the overall picture for both is the same. It is important to stress that the legend with the labelling of the subbands of the fQW for both graphics, follows our criterion for the sake of a proper comparison of the subbands in both, their and our calculations. Figure 2b shows the six first hole subbands for a GaAs iQW of 78 Å along $\langle 10 \rangle$ in-plane direction. The LH1-HH3 "anti-crossing" occurs at $\kappa_T = 0,035761$Å^{-1}. These results were compared with those obtained in [7] and the agreement was good for the corresponding states. It is im-

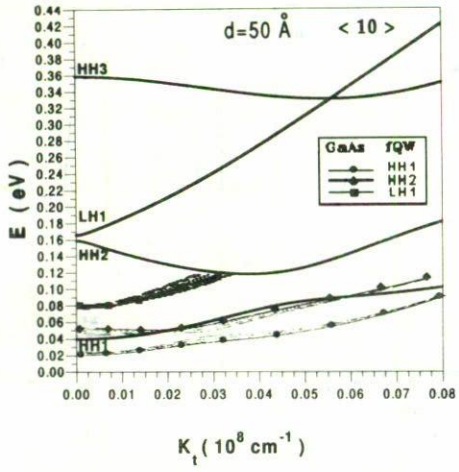

(a)

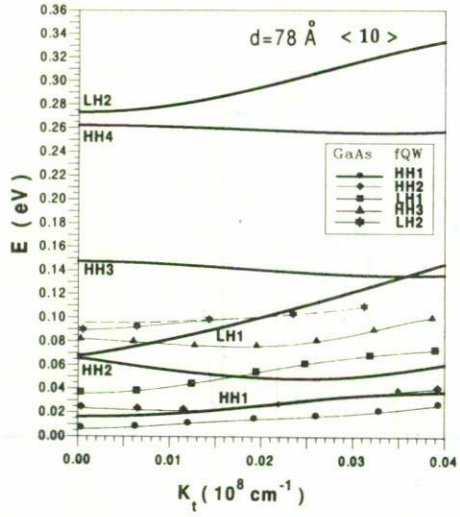

(b)

FIGURE 2. a) Dispersion of the first four valence subbands in a GaAs iQW of 50 Å along the ⟨10⟩ in-plane direction. Full lines correspond to our results, dashed lines correspond to curves for different values of the magnetic field. These results were taken from Ref. 12; b) Dispersion relation of the first six subbands in a GaAs iQW of 78 Å. Full lines refer to our results, different symbols were used for the results given in Ref. 7 for a fQW.

portant to note that the HH4 subband stands below LH2 in our result and does not appear in theirs. That result also agrees with that obtained by Chang and Schulman along the [100] direction and derives from expression (31). For both graphics (a) and (b) some comments must be done: The Γ point is a singular one because both heavy and light holes are degenerate and some formalism like that of the FTM fails down. Using the iQW case at this point one is allowed to obtain independent series (31) for HH and LH states, which unambiguously define the sequence of them although with a certain overestimation of their values. Is this fact, which makes relevant the use of this model. Beside that, the finiteness of the hole-barrier potential is not a strong enough condition to rear-

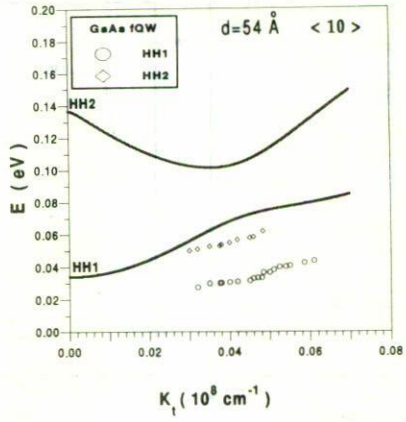

FIGURE 3. Dispersion of the two lowest valence subbands in a GaAs iQW of 54 Å. The full lines show the present calculated dispersion. Open circles and rhombus show the dispersion values corresponding to a hot-electron acceptor luminescence experiment for a GaAs-$Al_{0.25}Ga_{0.75}As$ QW given in Ref. 21.

range the states. So the iQW approach is expected to be significantly easier to deal with.

The LH1-HH3 anti-crossing appears in our calculations like a zero-gap degeneracy and in Ref. 6 it appears with a minigap. Leaving aside questions of numerical feasibility of the computing methods used to overcome that difficulty, we think that this is due to limitations of our model in which, on the first hand, the $\kappa \cdot \mathbf{p}$ basis is not complete (truncated) and, in the other, some linear k terms in the Hamiltonian (1) are neglected [4].

In Fig. 3 the first two subbands for a 54 Å QW are shown together with the experimental results of hole dispersion bands in a fQW determined by hot electron acceptor luminescense [21]. Even though our model does not take account directly of the spin split band and the infinite barrier approximation has been made, a reasonable semi-quantitative agreement is obtained-note that the energy differences are of a few millielectron volts.

Figure 4 show the components of the square modulus of the wavefunction of the states in subspaces U and L for the 4 lower hole states at the Γ point in an iQW of 50 Å. The curves labeled 1(3) are the HH components of the U(L) subspace and curves 2(4) the LH components. Also curves of the U(L) subspaces are depicted in solid(dashed) line. As can be seen, the curves of both subspaces coincide and have IC symmetry.

Figure 5 shows the components of the square modulus of the wavefunction of the U(L) subspace of the 4 lower hole states at $\kappa_T = 0.01\,\text{Å}^{-1}$. Curves labeled 1 (also with dashed line) and 3 (also solid line) are the HH components of the U and L subspaces respectively. The same occurs for curves 2 (also dashed line) and 4 (also solid line) for the LH components. They show lack of symmetry and the complementary shifting, although the shift form one curve to the other is not too big due to the fact that κ_T is near the Γ point.

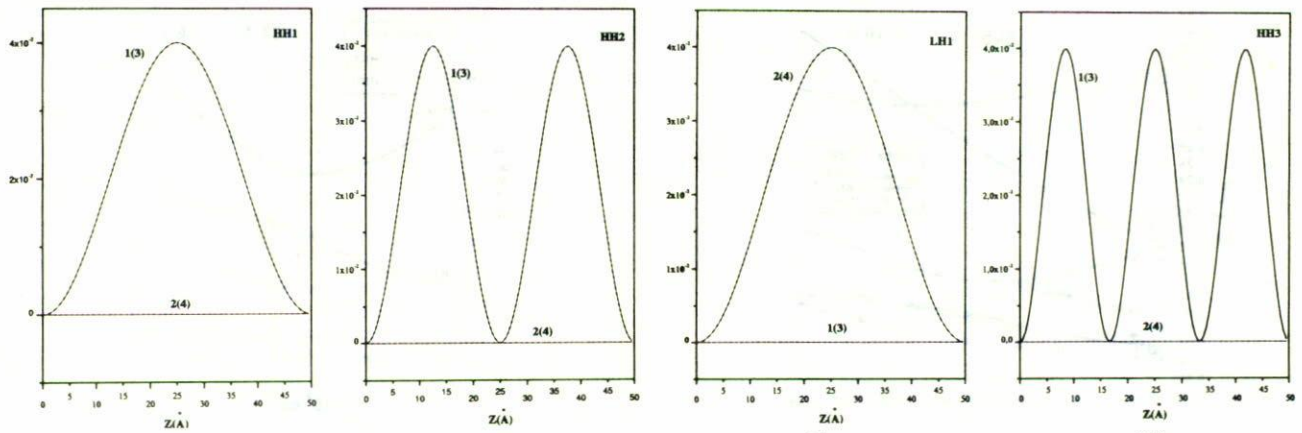

FIGURE 4. Components of the square modulus of the wavefunction of the hole states HH1, HH2, LH1 and HH3 at the Γ point in a 50 Å QW. Curves 1(3) are contributions of HH components for both U and L sub-spaces and curves 2(4) are the LH contributions.

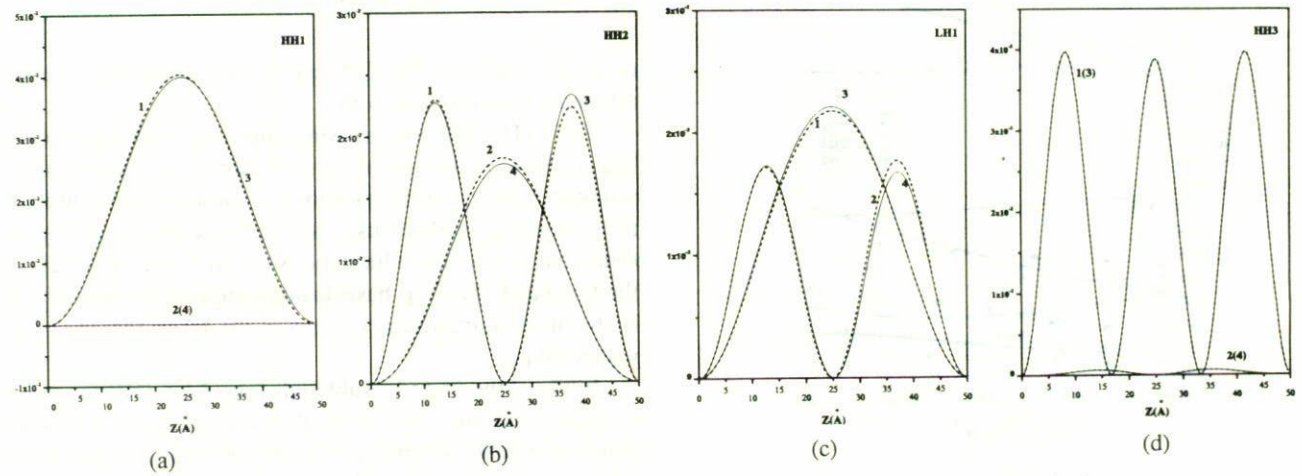

FIGURE 5. Components of the square modulus of the wavefunction of the same states as Fig. 4 at $\kappa_T = 0.01$ Å^{-1}. Curves labeled 1(3) are the HH contributions of the up (low) sub-space and curves 2(4) are the same for the LH contributions.

Figure 6 shows the components of the square modulus of the wavefunction of the LH1 and HH3 states at two different points of the Brillouin Zone, one just before and the other just after the point of accidental degeneracy depicted in Fig. 2a, to see whether this point is a crossing or anticrossing point. Figures 6a and 6b at the point $\kappa_T = 0.05440$ Å^{-1} and Fig. 6c and 6d the same states at the point $\kappa_T = 0.06$ Å^{-1}. The LH1 state must have one contribution with one zero and the other without any and, as can be seen, the dominant one is that with a zero which must be identified with HH. This behaviour occurs for both points in the Brillouin Zone. On the other hand, the HH3 state must have a contribution with two zeros and the other with one. The HH contribution is dominant in both k_T points. For the point after the degeneracy the energy which seems to be the HH3 subband has its contributions as expected for the LH1 subband and the contrary happens to the energy that seems to be LH1. This supports the statement that this accidental degeneracy point is an anticrossing with zero gap, in correspondence with the general arguments given above. We conjecture that the zero value for the gap is due to the incompleteness of the $\kappa \cdot \mathbf{p}$ basis considered.

6. Conclusions

The dispersion relation for the iQW of GaAs has been calculated for the KL model Hamiltonian using the TM method, with good agreement comparing our results with those obtained by other methods of calculation. An interchange in the labelling of the states was found in several authors with respect of the labelling which suggests series (31), which in turn agrees with that given in Ref. 6.

The discrete symmetries of the KL Hamiltonian for a symmetric QW in the basis most commonly used were described. This basis allows for a reduction in the number of equations to deal with (one of the sub-spaces U and L). The

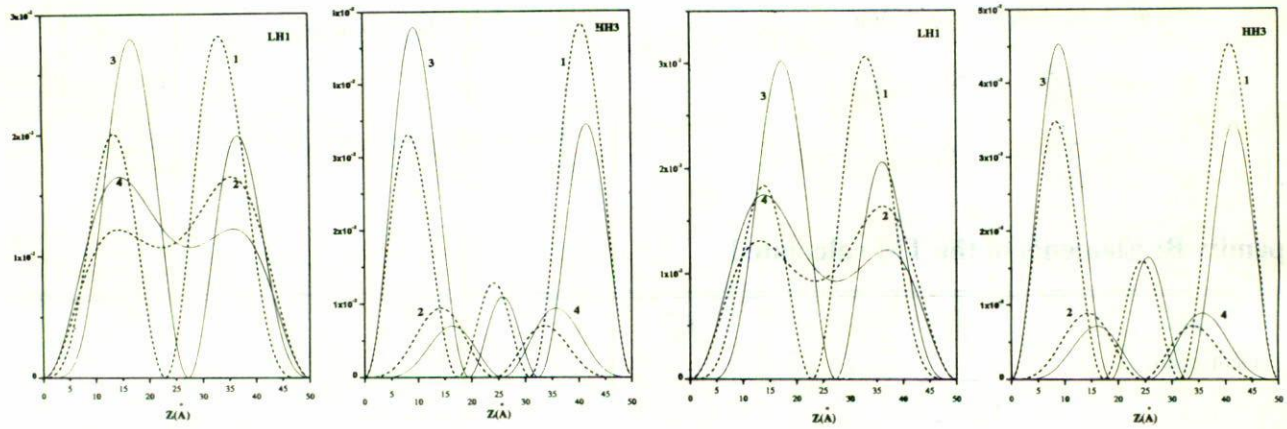

(a) (b) (c) (d)

FIGURE 6. (a) and (b) components of the square modulus of the wavefunction of the HH and LH contributions for the LH1 and HH3 states at the point $\kappa_T = 0.05440$ Å^{-1} for the same QW of Fig. 4; (c) and (d) are the same for the point $\kappa_T = 0.06$ Å^{-1}, *i.e.*, before and after the accidental degeneracy point.

lack of the symmetry under IC for the states of the sub-spaces at $\kappa_T = 0$ was shown both analytically and numerically, by evaluating the square of the wavefunction of those states, although the whole 4×4 state keeps this symmetry. With this evaluation the confirmation of an anti-crossing of the accidental degeneracy point of HH3 and LH1 subbands is borne out, in agreement with [6] and general symmetry arguments. Nevertheless, at $\kappa_T = 0$ the absence of coupling of the bands leads to satisfying IC symmetry at each sub-space. Physically speaking, the Γ point is singular for this Hamiltonian since at this point the bands are decoupled and the states have definite parity as "isolated systems" in this point. Once one moves away from this point, the coupling between bands is connected, the system is no longer isolated and then does not keep the parity defined in each 2×2 subspace.

The strategy "follow the box" for the numerical evaluation of a dispersion relation strongly nonlinear and complex valued is practical and efficient to overcome the numerical difficulties.

The extension to the case of fQW is straightforward and the labelling of the states using the series of the iQW at Γ point is still valid since the reduction of the height of the barriers is not sufficiently strong to change the order of appearance of the first states at this point of the Brillouin zone.

Acknowledgments

The authors are grateful J.A. Otero and A. Alvarez-Mesquida from ICIMAF, Cuba for computational support. We thank F. García-Moliner and V. Velasco-Rodríguez for valuable discussions and the first for a critical reading of the manuscript. One of the authors (H.R.-C.) is gratefully indebted for the hospitality of the Universitat Jaume I (Castellón, Spain) where part of this work was completed during the tenure of a Sabbatical Grant SAB1995-0733 of the Spanish Ministry of Education and Culture. This work has been supported partially by the UAM-A, D.F., and CONACyT of México under project No. 29026-E.

Appendix A: Parameters of the KL Hamiltonians

$$P = \frac{\hbar^2}{2m_0}\gamma_1(\kappa^2 + k_z^2); \qquad Q = \frac{\hbar^2}{2m_0}\gamma_2(\kappa^2 - 2k_z^2)$$

$$R = \frac{\hbar^2\sqrt{3}}{2m_0}(\mu k_+^2 - \gamma k_-^2); \qquad S = \sqrt{3}\frac{\hbar^2}{2m_0}\gamma_3 k_- k_z$$

$$T = -\frac{\hbar^2}{2m_0}\beta k_-; \qquad T' = -\frac{2}{\sqrt{3}}\frac{\hbar^2}{2m_0}\beta k_z$$

$$k_\pm = k_x \pm i k_y; \qquad k_T^2 = k_x^2 + k_y^2$$

$$\gamma = \frac{1}{2}(\gamma_2 + \gamma_3); \qquad \mu = \frac{1}{2}(\gamma_3 - \gamma_2)$$

$$A_1 = \frac{\hbar^2}{2m_0}(\gamma_1 + \gamma_2); \qquad A_2 = \frac{\hbar^2}{2m_0}(\gamma_1 - \gamma_2)$$

$$B_1 = \frac{\hbar^2}{2m_0}(\gamma_1 + 2\gamma_2); \qquad B_2 = \frac{\hbar^2}{2m_0}(\gamma_1 - 2\gamma_2)$$

$$C_{xy} = \sqrt{3}\,\frac{\hbar^2}{2m_0}\,\sqrt{\gamma_2^2(k_x^2 - k_y^2)^2 + 4\gamma_3^2 k_x^2 k_y^2};$$

$$D_{xy} = \sqrt{3}\,\frac{\hbar^2}{m_0}\,\gamma_3\,\kappa$$

$$a_1 = \gamma_1 + \gamma_2; \qquad a_2 = \gamma_1 - \gamma_2$$

$$b_1 = \gamma_1 + 2\gamma_2; \qquad b_2 = \gamma_1 - 2\gamma_2$$

$$q_i = k_i a_0 \quad i = x, y, z$$

$$q_T^2 = q_x^2 + q_y^2; \qquad q = \lambda a_0$$

$$t_{xy} = \frac{C_{xy}}{Ry}; \qquad S_{xy} = \frac{D_{xy}}{Ry}$$

$$\tilde{\mathcal{E}} = \frac{\mathcal{E}}{Ry}; \qquad V_0 = 0$$

$$\beta_T = \frac{1}{2}\left[(a_1 b_1 + a_2 b_2) q_T^2 + (b_1 + b_2)\tilde{\mathcal{E}} - S_{xy}^2\right];$$

$$\alpha_T = b_1 b_2$$

$$\delta_T = a_1 a_2 q_T^4 + (a_1 + a_2)\tilde{\mathcal{E}} q_T^2 + \tilde{\mathcal{E}}^2 - t_{xy}^2$$

Appendix B: Elements of the TM calculated

Matrix elem. coeff.	$\ell_{ij}^{(1)}$	$\ell_{ij}^{(2)}$	$\ell_{ij}^{(3)}$	$\ell_{ij}^{(4)}$
M_{11}	$b_2 q_1 \alpha_1 \Omega_3$	$-b_2 q_1 \alpha_2 \Omega_1$	$\alpha_1 \alpha_2 t_{xy} S_{xy}$	$-\alpha_1 \alpha_2 \frac{q_1}{q_3} t_{xy} S_{xy}$
M_{12}	$-b_2 q_1 \alpha_1 \alpha_2 t_{xy}$	$b_2 q_1 \alpha_1 \alpha_2 t_{xy}$	$-S_{xy}\Theta_2$	$-\frac{q_1}{q_3} S_{xy}\Theta_2$
M_{13}	0	0	$\alpha_1 \Theta_1$	$-\frac{q_1}{q_3}\alpha_2 \Theta_1$
M_{14}	$-b_2 q_1 \alpha_1 \alpha_2 S_{xy}$	$b_2 q_1 \alpha_1 \alpha_2 S_{xy}$	$-b_2 \alpha_1 \alpha_2 t_{xy}$	$\frac{q_1}{q_3} b_2 \alpha_1 \alpha_2 t_{xy}$
M_{21}	$q_1 t_{xy}\Theta_3$	$-q_1 t_{xy}\Theta_1$	$S_{xy}\Theta_4$	$-\frac{q_1}{q_3} S_{xy}\Theta_4$
M_{22}	$-\alpha_2 q_1 \Theta_1$	$\alpha_1 q_1 \Theta_1$	$-S_{xy} t_{xy} \alpha_1 \alpha_2$	$\frac{q_1}{q_3} S_{xy} t_{xy} \alpha_1 \alpha_2$
M_{23}	$-q_1 S_{xy}\Theta_1$	$q_1 S_{xy}\Theta_1$	$t_{xy}\Theta_1$	$-\frac{q_1}{q_3} t_{xy}\Theta_1$
M_{24}	0	0	$-b_2 \alpha_2 \Omega_1$	$b_2 \alpha_1 \Omega_3 \frac{q_1}{q_3}$
M_{31}	$q_1 \alpha_1 \alpha_2 S_{xy} t_{xy}$	$-q_1 \alpha_1 \alpha_2 S_{xy} t_{xy}$	$-b_2 q_1^2 \alpha_1 \Omega_3$	$b_2 q_1 q_3 \alpha_2 \Omega_1$
M_{32}	$-q_1 \alpha_1 \alpha_2 S_{xy}\Theta_2$	$q_1 \alpha_1 \alpha_2 S_{xy}\Theta_2$	$b_2 q_1^2 \alpha_1 \alpha_2 t_{xy}$	$-b_2 q_1 q_3 \alpha_1 \alpha_2 t_{xy}$
M_{33}	$\alpha_1 q_1 \Theta_1$	$-\alpha_2 q_1 \Theta_1$	0	0
M_{34}	$-b_2 q_1 \alpha_1 \alpha_2 t_{xy}$	$b_2 q_1 \alpha_1 \alpha_2 t_{xy}$	$b_2 q_1^2 \alpha_1 \alpha_2 S_{xy}$	$-b_2 q_1 q_3 \alpha_1 \alpha_2 S_{xy}$
M_{41}	$q_1 S_{xy}\Theta_4$	$-q_1 S_{xy}\Theta_4$	$-q_1^2 t_{xy}\Theta_3$	$q_1 q_3 t_{xy}\Theta_1$
M_{42}	$-q_1 \alpha_1 \alpha_2 S_{xy} t_{xy}$	$q_1 \alpha_1 \alpha_2 S_{xy} t_{xy}$	$\alpha_1 q_1^2 \Theta_1$	$-q_1 q_3 \alpha_1 \Theta_1$
M_{43}	$q_1 t_{xy}\Theta_1$	$-q_1 t_{xy}\Theta_1$	$\alpha_2 q_1^2 \Theta_1$	$-\alpha_1 q_1 q_3 \Theta_1$
M_{44}	$-b_2 q_1 \alpha_2 \Omega_1$	$b_2 q_1 \alpha_1 \Omega_3$	0	0

Some parameters used in the above table are:

$$\alpha_1 = b_2 q_1^2 + \Theta_2; \qquad \alpha_2 = b_2 q_3^2 + \Theta_2$$

$$\Delta_T = b_2 q_1 (q_1^2 - q_3^2)\Theta_1$$

$$\Theta_1 = b_2 t_{xy}^2 - \Theta_2 S_{xy}^2; \qquad \Theta_2 = a_1 q_T^2 + \tilde{\mathcal{E}}$$

$$\Theta_3 = b_2 \Omega_3 - \alpha_2 S_{xy}^2; \qquad \Theta_4 = b_2 q_1^2 \Omega_3 + \alpha_2 t_{xy}^2$$

$$\Omega_1 = t_{xy}^2 + q_1^2 S_{xy}^2; \qquad \Omega_3 = t_{xy}^2 + q_3^2 S_{xy}^2$$

1. E.P. O'Reilly and G.P. Witchlow, *Phys. Rev. B* **34** (1986) 6030.
2. G. Schechter, L.D. Shvartsman, and J.E. Golub, *J. Appl. Phys.* **78** (1995) 288.
3. S.S. Nedorezov, *Fiz. Tverd. Tela* **12** (1970) 2269; [*Sov. Phys. Solid State* **12** (1971) 1814].
4. D.A. Broido and L.J. Sham, *Phys. Rev. B* **31** (1985) 888.
5. J.N. Schulman and Yia-Chung Chang, *Phys. Rev. B* **31** (1985) 2056.
6. Yia-Chung Chang and J.N. Schulman, *Phys. Rev. B* **31** (1985) 2069.
7. L.C. Andreani, A. Pasquarello, and F. Bassani, *Phys. Rev. B* **36** (1987) 5887.
8. U. Ekenberg, L.C. Andreani, and A. Pasquarello, *Phys. Rev. B* **46** (1992) 2625.
9. Z. Ikonić and V. Milanović, *Phys. Rev. B* **45** (1992) 8760.

10. Z. Ikonić, V. Milanović, and D. Tjapkin, *Phys. Rev. B* **46** (1992) 4285 .
11. A.D. Sánchez and C.R. Proetto, *J. Phys. Condens. Matter* **7** (1995) 2059.
12. G. Goldoni and A. Fasolino, *Phys. Rev. B* **51** (1995) 9903.
13. M.E. Mora, R. Pérez-Alvarez, and Ch.B. Sommers, *J. Physique* **46** (1985) 1021.
14. R. Pérez-Alvarez and H. Rodríguez-Coppola, *Phys. Stat. Sol. (b)* **145** (1988) 493.
15. H. Rodríguez-Coppola, V.R. Velasco, R. Pérez-Alvarez, and F. García-Moliner, *Phys. Scripta* **53** (1996) 377.
16. R. Wessel and M. Altarelli, *Phys. Rev. B* **34** (1989) 12802.
17. G.L. Bir and G.E. Picus, *Symmetry and Strain-Induced Effects in Semiconductors*, (Wiley, New York, 1974). (In Russian).
18. V.L. Bonch-Bruevich and S.G. Kalashnikov, *The Physics of Semiconductors*, (Nauka, (Moskow), 1990). (In Russian).
19. A. Alvarez-Mesquida and J.A. Otero, *private communication.*
20. M.F.H. Schuurmans and G.W. 't Hooft, *Phys. Rev. B* **31** (1985) 8041.
21. M. Zachau, J.A. Kash, and W.T. Masselink, *Phys. Rev. B* **44** (1991) 4048.
22. C. Weisbush and B. Vinter, *Quantum Semiconductor Structures* (Academic Press, San Diego, 1991).
23. W.H. Press, S.A. Teutolsky, W.T. Vetterling, and B.P. Flannery, *Numerical Recipies*, (Cambridge University Press, London, 1992).